SUPPLEMENTAL MATERIAL

1. Statistical data analysis

To capture bumblebee flights only, we exclude any crawling behavior on the landing platforms by also removing all data within a 1 cm boundary region of each platform. The size of this boundary is based on the size of the bumblebees, which have a height of approximately 1 cm. While smaller cutoffs would not exclude all crawling behavior, the cutoff can be increased robustly within reasonable bounds. We have checked that, e.g. a 2 cm cutoff does not have any influence on any of the analyzed quantities, as the amount of the data which would be excluded in addition is very small. This leaves from 2000 to 15000 data points (average: 6000) per bumblebee for each stage. We select the best model for the velocity distributions by maximum likelihood estimation and Akaike and Bayesian weights for our candidate distributions [16] for $|v| \geq 2.5\,\mathrm{cm/s}$. Given a set of measured velocities $D = \{v_1, v_2, ..., v_n\}$ and a probability density function $\rho_\lambda(v)$, where λ is a vector of k parameters, the *log-likelihood* of the probability density function for a finite resolution of the data ($\Delta v = 5\,\mathrm{cm/s}$) simplifies to

$$\ln L(\lambda|D) = \sum_{v_j \in D} \ln P_\lambda(v_j) = \sum_{b \in bins} h[b] \ln \int_{min(b)}^{max(b)} \rho_\lambda(v) dv$$

where $h(b)$ is the observed frequency in bin b.

For each candidate distribution $\rho^i_{\lambda_i}$, $i \in \{1, 2, 3\}$, we maximize the log-likelihood $\ln L_i$ w.r.t. λ_i locally with a Nelder-Mead algorithm by using a Monte Carlo method to find the global maximum. To find the preference between the different model distributions whose likelihoods L_i are maximized at λ_i^{max} the information criteria are

$$IC_i = -2\ln(L_i(\lambda_i^{max}|D)) + s(n)k_i$$

with $s(n) = 2$ for the Akaike information criterion and $s(n) = \ln(n)$ for the Bayesian information criterion as a penalty on the number of parameters k_i. The best model, denoted by $*$, is the one which minimizes the information criterion $IC_* = \min_i(IC_i)$. The Akaike/Bayesian weights then give the preference of each model over the others as a probability

$$w_i = \alpha \mathrm{e}^{-(IC_i - IC_*)/2} ,$$

where α normalizes the weights to $\sum_i w_i = 1$.

The choice of the information criterion makes no strong difference for the model selection in this experiment. With the Akaike information criterion the Gaussian mixture is chosen with a weight of over 95% for all bumblebees and all experimental stages. The Bayesian information criterion agrees with the Akaike information criterion on 90% of all data sets. For the other 10% it prefers a single Gaussian or an exponential distribution - these data sets turned out to be those with the least amount of data available.

To compute the autocorrelation function $v^{ac}(\tau)$ of the flight velocities

$$v^{ac}(\tau) = \frac{\langle (v(t) - \mu)(v(t+\tau) - \mu) \rangle}{\sigma^2}$$

we average over all bumblebees and over time in all flights that are complete from starting on one flower to landing on the next. We exclude flights containing gaps and correlation terms, where in-between time t and $t + \tau$ a flower was visited.

Table I. Model weights and estimated parameters. Akaike and Bayesian weights both give preference to the mixture of two Gaussians for v_y for most of the bumblebees. The weights are estimated individually and their mean and standard deviation (in brackets) are shown. The distribution parameters are also estimated individually for each bumblebee in each stage.

Model:	(a) Exponential	(b) Power law	(c) Gaussian	(d) Gaussian Mixture		
Akaike weight	0.00 (0.00)	0.00 (0.00)	0.04 (0.19)	0.96 (0.19)		
Bayesian weight	0.04 (0.18)	0.00 (0.00)	0.08 (0.26)	0.88 (0.30)		
Parameters	λ	μ	σ	a	σ_1	σ_2
average (bumblebees)	5.61	1.11	0.25	0.67	0.06	0.29
stddev (bumblebees)	1.07	0.16	0.03	0.13	0.04	0.03

Table II. Weights and estimated parameters of the Gaussian mixture for the different experimental stages. Weights and parameters are estimated for each bumblebee. Shown are the mean over all individuals and the standard deviation (in brackets). The mixture of two Gaussians is the best fit in all stages. In the parameters of the distribution we observe no significant effect of the threat of predators on the bumblebees.

Stages	Akaike weight	Bayesian weight	a	σ_1	σ_2
(1) Without spiders	0.97 (0.15)	0.93 (0.23)	0.64 (0.11)	0.06 (0.02)	0.29 (0.03)
(2) Under predation risk	0.99 (0.04)	0.90 (0.27)	0.68 (0.13)	0.06 (0.02)	0.29 (0.02)
(3) With risk, 1 day later	0.89 (0.29)	0.80 (0.38)	0.72 (0.16)	0.07 (0.07)	0.30 (0.03)

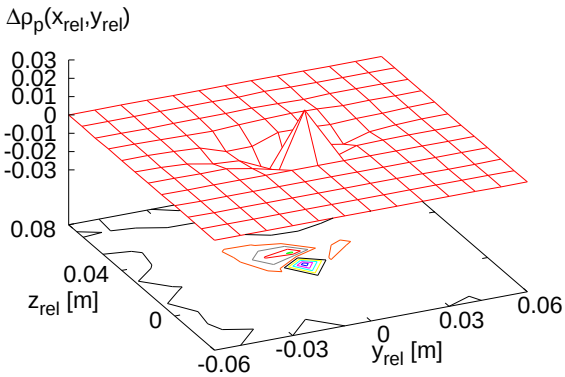

Figure S1. Predator avoidance of bumblebees at flowers, Eq. (1), extracted from the experimental data. Hovering behavior in front of a flower is represented by the positive spike directly at the flower center, while the negative region behind this spike reflects the avoidance in the flights towards a flower.

2. Mathematical modeling of bumblebee foraging

The effect of the presence of a spider on the probability of a bumblebee to fly in front of a flower can be measured by computing the difference between the position densities at stage (1) and (2) as a function of the positions parallel to and near (x <5 cm) the flower wall,

$$\Delta\rho_p(y_{rel}, z_{rel}) = \rho_p^{(2)}(y_{rel}, z_{rel}) - \rho_p^{(1)}(y_{rel}, z_{rel}) \,, \quad (1)$$

where the positions (y_{rel}, z_{rel}) are relative to the nearest flower center. This predator avoidance extracted from the experimental data is shown in Fig. S1. Two different types of behavior can be seen: First, there is a small increase in the amount of hovering, i.e. inspection flights near the flower platform when a spider model is present [1, 2], which is consistent with Ref. [3]. However, more important is the local minimum representing the avoidance of flowers infected by spiders. This effect is strongest 3 cm above the dangerous flowers, because the flowers are predominantly approached from above. The avoidance behavior affects not only flights near the flower wall but can still be detected further away from it. Comparing dangerous and safe flowers at stage (2) only confirms that avoidance is the dominant effect for search flights.

The avoidance of spider-infected flowers together with the spatial switching of flight modes discussed in the main part of our Letter can be modeled by the Langevin Equation

$$\begin{aligned} \frac{d\mathbf{r}}{dt}(t) &= \mathbf{v}(t) \\ \frac{d\mathbf{v}}{dt}(t) &= -\eta\mathbf{v}(t) - \nabla U(\mathbf{r}(t)) + \xi(\mathbf{r}, t) \,, \end{aligned} \quad (2)$$

where η is a friction coefficient and ξ white Gaussian noise with standard deviation depending on the flight mode as a function of the position, $\xi(\mathbf{r}, t) = \chi_{\mathsf{fz}}(\mathbf{r})\xi_1(t) + (1 - \chi_{\mathsf{fz}}(\mathbf{r}))\xi_2(t)$. Here $\mathbf{r} = (x, y, z)^\top$ is the position of the bumblebee at time t, $\chi_{\mathsf{fz}}(\mathbf{r})$ is the indicator function of the feeding zone, which is equal to one whenever the bumblebee is in the cube around a flower as defined before, and ξ_i , $i = 1, 2$ is Gaussian noise with two different variances. The potential U models an interaction between bumblebee and spider in form of a repulsive force exerted by the spider onto the bumblebee, for which we assume that the potential maxima are located near infected flowers.

When the mechanism generating the correlation functions shown in Fig. 3 is not the focus of the investigation, it suffices to consider a reduced version of Eqs. (2) in form of the *effective* Langevin equation

$$\frac{d\mathbf{r}}{dt} = \chi_{\mathsf{fz}}(\mathbf{r})\zeta_1(t) + (1 - \chi_{\mathsf{fz}}(\mathbf{r}))\zeta_2(t) \,. \quad (3)$$

This equation describes the spatially varying hovering and search modes by using noise ζ_i , $i = 1, 2.$, which models the impact of the potential U together with the noise ξ. Further data analysis shows that excluding hovering has no significant impact on the velocity autocorrelations, which are dominated by the search flights. This is in full agreement with Fig. 3, where the time scale for the predator-induced anti-correlation (Fig. 3(b)) is larger than the time scale for flights between neighbouring flowers (Fig. 3(a)). Hence, we model $\zeta_1(t)$ as a vector of Gaussian white noise with the smaller variance σ_1^2 given in Table I which describes the hovering. The search flights from flower to flower are reproduced by the correlated Gaussian noise vector $\zeta_2(t)$ with variance σ_2^2 and the autocorrelations $v_i^{ac}(\tau)$, $i = x, y$ shown in Fig. 3. The advantage of this model is that it is directly based on our data analysis.

We now focus on the different aspect of understanding the biophysical mechanism that generates the anti-correlations of the velocities parallel to y shown in Fig. 3(b). Starting from the full model Eqs. (2), it suffices to select the search mode only by setting $\xi(\mathbf{r}, t) = \xi_2(t)$ thus neglecting any spatial variations of the noise. This yields the Langevin equation

$$\frac{dv_y}{dt}(t) = -\eta v_y(t) - \frac{\partial U}{\partial y}(y(t)) + \xi(t) \,, \quad (4)$$

which was already stated in the main part as the main equation. A rough approximation for the repulsive force is provided by a periodic potential with maxima at dangerous flowers,

$$U(\mathbf{r}) = u \cos\left(2\pi \frac{y}{y_0}\right) \,, \quad (5)$$

where y_0 is the mean distance between spiders and u the strength of the repulsion.

We integrated this Langevin equation via an Euler-Maruyama method under variation of u by computing the autocorrelation function v_y^{ac} of the generated data. Figure S2 shows v_y^{ac} by increasing the repulsion strength u. The correlation function changes from positive correlations to anti-correlations in a range of delay times τ comparable to the changes in the correlation function of the experimental data of Fig. 3(b). This qualitatively reproduces our experimental findings from first principles. Note that the oscillations for higher

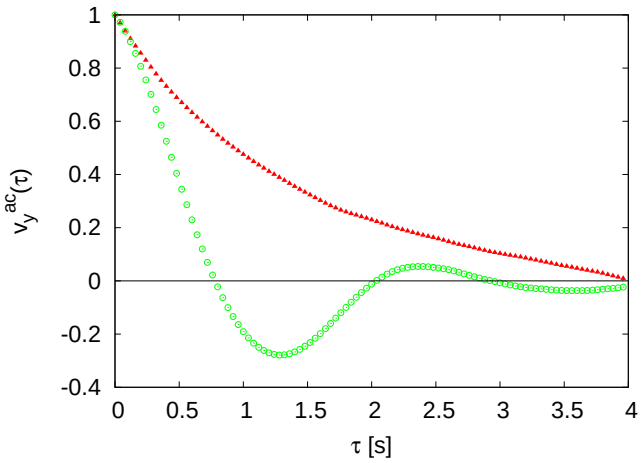

Figure S2. Autocorrelation function of the velocities v_y for the Langevin model Eqs. (4),(5) modeling predation threat by different strengths of a repulsive potential. Shown are results from computer simulations without ($u = 0$; red triangles, upper line) and with predation threat ($u = 0.5\,\mathrm{m}^2/\mathrm{s}^2$; green circles, lower line). These results should be qualitatively compared with the experimental findings Fig. 3(b).

τ in Fig. S2 would be suppressed in a higher-dimensional model. The other directions can be treated analogously, e.g., by including an x-dependent term in the potential for the attraction of the bumblebees to the flower wall. A stochastic analysis of Langevin equations with periodic potentials can be found, e.g., in Ref. [4]. The effect of the harmonic potential on the creation of negative velocity correlations can also be calculated analytically [5].

We emphasize that our model Eqs. (4),(5) provides only a qualitative description of the biophysical mechanism generating the change in the correlations of the bumblebee velocities under predation threat. For a quantitative comparison to the experimental data a much more detailed model would be necessary, which needs to include the random positioning of the spiders and the general attractive force exerted by the flowers onto the bumblebees. Modeling the three-dimensional nature of the potential would also be important: Notice, e.g., the local maximum of v_y^{ac} around $\tau \simeq 2.5$ which is an artifact of the one-dimensional modeling of spider avoidance. However, as it is difficult to reliably estimate the parameters of the potential, such a quantitative comparison is beyond the scope of our Letter.

[1] T. Ings, M. Y. Wang, and L. Chittka, Behavioral Ecology and Sociobiology, 1 (2011).

[2] T. Yokoi and K. Fujisaki, Naturwissenschaften, **96**, 195 (2009).

[3] T. C. Ings and L. Chittka, Current Biology, **18**, 1520 (2008).

[4] H. Risken, *The Fokker-Planck Equation : Methods of Solution and Applications* (Springer, Berlin New York, 1989).

[5] F. Lenz, A. V. Chechkin, T. C. Ings, L. Chittka, and R. Klages, In preparation.